A Novel Water Based Cooling Approach to Increase Solar Panel Efficiency

Thesis

Nicholas Giza

Advisor: Dr. Kevin Crowthers, Ph.D.

The Massachusetts Academy of Math and Science

Worcester, Massachusetts, The United States of America

Abstract

As the world becomes increasingly more dependent on its power grids, it has simultaneously become more dependent on fossil fuels. To offset this harmful reliance, photovoltaic solar panels (PVs), can be used to cleanly and renewably produce electricity. One major flaw that plagues solar energy is the fact that PVs lose significant amounts of efficiency when hot. In fact, for every 1℃ increase in temperature (above 25℃), there is a 0.08% to 0.45% drop in power output efficiency (Alktranee & Péter, 2023). With normal operating temperatures as high as 70℃ (Akal & Türk, 2022), this is detrimental to electrical output. In response, this study produced a closed-loop, water-cooling system powered by thermoelectric generators (TEGs) to reduce solar panel temperatures and increase performance. Two forms of apparatus were designed and analyzed. Finite element analysis in SolidWorks simulated coolant flow and served as a visual representation for to-scale design. FEM results were tested in a physical environment where one control PV and one water-cooled PV-TEG were set up under a 1728W array of halogen light bulbs. In testing, SolidWorks Flow Simulations suggested relatively equitable coolant flow rates, supported with f-tests. Physical testing suggested a 4.70W or 10.18% average increase in efficiency/power output; enough power, when scaled to a fully powered PV, to support the cooling system. With this in mind, entire solar array cooling systems can be designed that scale this system accordingly. The implications of this highly functional, closed-loop cooling system for PVs provide immense potential for a more sustainable planet.

Keywords: Photovoltaic Cooling, Thermoelectric Generators, Efficiency, Flow Simulation, Solar Simulator

A Novel water-based Cooling Approach to Increase Solar Panel Efficiency

As populations rise and technology advances, there is a continuous need for more energy. Unfortunately, that often means using more fossil fuels to offset the increased global power draw. Fossil fuels are actively destroying the environment through the emission of greenhouse gasses including carbon dioxide. As a result, it is paramount to our planet's well-being that advances be made to increase the output of renewable energy sources, such as solar, to reduce dependence on fossil fuels. Solar energy is a form of clean, renewable energy that uses photovoltaic cells to convert solar radiation into electrical energy. This process releases no greenhouse gasses and is a popular option for those looking to reduce their dependence on fossil fuels and, consequently, reduce their carbon footprint.

Only about 15% of the solar irradiance[1] that reaches solar panels is converted to energy; the rest is lost as heat (Salehi et al., 2021). As the solar panels heat up, they lose a significant magnitude of power output. In fact, for every 1℃ increase in temperature (above 25℃), there is a 0.08 to 0.45 percent drop in power output efficiency (Alktranee & Péter, 2023). With normal operating temperatures as high as 70℃, this is detrimental to electrical output (Akal & Türk, 2022). Thus, high operating temperatures are a significant threat to the efficiency of PVs. Panels operate at the lowest possible temperatures to produce the most electricity. If more energy can be harvested by solar, less fossil fuels must be burned to support power grids worldwide.

Previous Research

Several studies have been conducted to address solar panel cooling, and they can be divided into two main categories: active cooling and passive cooling. Active cooling requires an input of electricity, whereas passive cooling does not. Previous studies have utilized various cooling methods

[1] Radiation that hits the surface of an object.

including water cooling (Chanphavong et al., 2022; Terashima et al., 2023; Zubeer & Ali, 2022), nanofluids, forced and passive air circulation (Rahman et al., 2023), thermoelectric modules (Salehi et al., 2021), heat sinks, and many others. While most studies with active water-cooling solutions use pumps to circulate coolant, few consider the associated power draws. Furthermore, fewer try to subsidize this power draw. A significant knowledge gap arises when thermoelectric generators are put into consideration. Thermoelectric generators convert heat flux (temperature differences) into electricity via the Seebeck effect (Jaziri et al., 2020). There is a clear lack of knowledge regarding how thermoelectric generators can work in conjunction with photovoltaic (PV) water cooling systems.

Researchers based in Laos, led by Lemthong Chanphavong, created an active cooling system consisting of a thin layer of continuously flowing water over the surface of a panel to keep it cool. Two solar panels were set up. One had no specialized cooling system, while the other had a custom water-cooling system. This system consisted of a few PVC pipes oriented so that a DC pump could transport water to the top of the panel. As the water left a distribution PVC pipe, it formed a thin, flowing film over the surface. During testing, climate conditions (ambient temperatures, relative humidity, wind speeds, and solar irradiances) as well as electrical outputs of the panels and panel surface temperatures were measured every thirty minutes. Results suggest an approximate exergy (usable energy) efficiency increase of 9.8% as a direct result of lowering panel temperatures by as much as 29.2℃ (Chanphavong et al., 2022).

A study in Japan, led by Terashima et al. (2023), aimed to compare two different water-based solar PV/T or photovoltaic thermal systems using both a CIS (copper, indium, selenium) and a m-Si (monocrystalline silicon) panel type. A water block was placed on the rear side of the panel, where flow rates were controlled to change the output temperature of the coolant. These output temperatures corresponded to two use cases: space heating and cooling. Instead of a traditional pumping method, a

decompression-boiling heat collector was used, boasting lower power draw, and higher efficiency. Results suggest that the CIS PV/T system was able to convert 73.5% of the solar energy at a 40℃ water output and 45.9% of the solar energy at a 60℃ water output, whereas the m-Si panel type, in the same conditions, showed to operate at a dramatically lower efficiency (Terashima et al., 2023).

A Malaysian research group, led by Noor Muhammad Abd Rahman, utilized a custom cooling system consisting of a customized plenum[2] and specially designed aluminum heat sinks to transport cool air from a heat pump through the back of the panel and back down to the heat pump where the heat can be recycled. The findings suggest an impressive 12.35% increase in panel efficiency (as compared to the nominal operating cell temperatures, NOCT) and a comparatively low, 17% decrease from the standard testing conditions (STC) (Rahman et al., 2023).

A research group, led by Salehi et al. (2021), studied the use of thermoelectric modules to pump heat from the rear of a solar panel to corresponding anodized aluminum heat sinks. This system reduced the overall temperature of the panel by an average of 10.04℃, allowing for a 10.50% increase in energy output (Salehi et al., 2021).

Similarly, another group researched the use of thermoelectric generators in improving solar efficiency by reducing panel temperatures and in turn producing electricity through the Seebeck effect. The Seebeck effect is a natural phenomenon that states that whenever there is a temperature difference between two different electrical semiconductors/conductors, a voltage is produced between those two materials. Thirty thermoelectric generators, fitted with aluminum heat sinks, were put on the back of a solar panel to reduce panel temps and increase output electricity. Results suggest an average of 8.4% more electrical energy was produced by the TEG than the standard PVs (Akal & Türk, 2022).

[2] An air intake device to direct airflow in a controllable manner.

According to research done by a group from the Indian Institute of Technology, operating temperatures of photovoltaic cells are crucial to their longevity. When the temperatures within the cells vary too significantly, delamination can occur, resulting in the deterioration and shortened lifespan of PV cells. To model this situation, a conduction-based thermal model was designed to analyze the thermal interactions between a PV with and without a rear-mounted heatsink. Results suggest that hotspots, which cause delamination, tend to occur on the outer edges of the PV. With the addition of a simple, passive cooling system, this model was able to find an approximate 1% increase in PV efficiency (Laha et al., 2021).

The proposed design works to include concepts from each of these studies including conduction-based water-cooling and the use of thermoelectric modules to effectively cool a PV system and in doing so, increase PV power output. The major reference designs are from Akal & Türk (2022) and Terashima et al. (2023) as both have influenced the design and methods of this project.

With the previous studies in mind, there are a few criteria that this model must conform to. Firstly, the solution should be relatively inexpensive as it would not make sense for practical application if it could not pay for itself with increases in PV efficiency. In conjunction with cost is effectiveness; this system must result in a notable net increase in overall PV efficiency. Next, the system must be relatively simple to produce and install, and able to be easily redesigned/adapted to various panels. Lastly, the system must not require a constant input of materials such as coolant or electricity to reduce operating expenses and maintain positive efficiency.

Problem Statements

1. Solar panels lose a considerable amount of efficiency when operating at heightened temperatures.

2. Common cooling solutions often consume a large sum of electricity, damaging the net efficiency.
3. PV hotspots created by cooling solutions can damage PV longevity.
4. Cooling systems are largely unavailable to the general public as a result of expense and complexity.

Objectives

There are currently no largely commercialized solutions for solar panel cooling and most real-world implementation that has been done to cool panels has been on a highly customized, costly, individualized basis, leaving a few objectives for this design to target.

Obj. 1a: It is aimed that this system effectively reduces the overall cell temperatures of the PV.

Obj. 1b: This cooling solution aims to increase the net output power of the PV as a result of lowered operating temperatures.

Obj. 1c: This design aims to equitably cool the PV, with relatively equal temperatures across the panel, reducing hotspot potential.

Obj. 2: Another major objective is to reduce or completely subsidize the overall power draw of the proposed cooling system with thermoelectric generators.

Obj. 3: A key objective in the design of this project was ensuring relatively equitable temperature distributions across the rear of the PV.

Obj. 4: This design aims to provide a relatively simple in design, lower-expense solution to PV cooling.

Significance of Solar Efficiency

Solar panel efficiency defines global sustainability. As of 2023, 3.4% or 144,000,000,000 KWh of the United States power is produced by solar. If solar panels can be made universally more efficient by even just 5%, the United States power grids could become 0.3% less dependent on fossil fuels such as petroleum. While this may not sound significant, roughly 3.1 million barrels of petroleum liquids would remain unburned annually, reducing carbon dioxide emissions by roughly 1.4 million metric tons per year (U.S. Energy Information Administration, 2023a). The effect on the planet and global CO2 emissions would be profound. Any improvement to the efficiency of PVs can be an improvement to the condition of the planet and the sustainability of the world's power grids.

Section 2: Methodology

2.1 Role of Student vs. Mentor

During the past five months, I was responsible for project brainstorming, research, and design, along with seeking out additional resources and assistance. The mentor of this project, Dr. Kevin Crowthers was responsible for ensuring proper documentation, consistent effort and adherence to deadlines while also defining the basic project deliverables and providing advice on seeking assistance. Further help was provided by Dr. Powell at the Worcester Polytechnic Institute who aided in thermal modeling and understanding of solar economics. The framework and overall design of the Arduino-based data collection system was designed with the help of Pavel Loven, an electrical engineer at Advanced Micro Devices and Shaun Lindgren from Lindgren Electric provided insight into electrical safety and design, while advising on the overall creation of the physical simulator.

2.2 Equipment and Materials

A wide variety of equipment was used to complete this project and can be divided into two categories: software and hardware. The softwares utilized include SolidWorks, TinkerCad and the Arduino IDE 2.2.1. SolidWorks was used to model the thermal interactions within the backplate, the Arduino IDE was used to run the data collection system in the physical simulation and CoolTerm was used to transcribe the Arduino results to a .txt file. TinkerCad was employed to design some of the custom components of the water block. The hardware that was utilized includes 2 Renogy 175W PVs, aluminum for building the backplate, halogen light bulbs (and respective wiring and dimmer switches) for providing radiant energy to the PV, chains for suspending the PV, multimeters for recording PV current and voltage, a 12V aquarium pump for coolant circulation, 10 TEGs for supplementing power to the pump, 10 aluminum heatsinks to reduce temperature of the TEGs' cold sides, and aluminum adhesive to hold the backplate together.'

2.3 Conceptual design

2.3.1 Rear mounted water loop

Several studies have examined the effectiveness of PV water cooling and have generally found water[3] cooling systems highly effective. Based on these studies, two categories of water cooling can be identified: closed loop and open loop. Closed loop water cooling systems are sealed off and, if built properly, will not lose an impactful quantity of coolant through normal operation. These systems require the water to be cooled after passing through the heat source to return and efficiently draw heat from a PV (Chanphavong et al., 2022; Terashima et al., 2023). If the coolant returns hot, it will have a weaker cooling effect as justified by the specific heat formula. Open loop cooling, on the other hand, does not

[3] Water and coolant will be used interchangeably throughout this paper as water is the coolant

necessarily reuse the coolant and often requires a constant water source and a method to dispose of used coolant. If used coolant is recirculated, it is generally more at risk to factors such as evaporation or contamination from outside elements such as dust or other debris (Zubeer & Ali, 2022; Alktranee & Péter, 2023). Consequently, open loop cooling systems often have a larger resource and maintenance requirement. With this in mind, a closed loop PV water cooling system was chosen for use in the proposed apparatus to take advantage of the cooling abilities of water while not requiring a considerable amount of maintenance or resource input.

To contain the water and effectively transport heat, an aluminum water block was used. Aluminum was chosen because it has a high specific heat capacity of 0.89 J/g°C and is able to effectively transfer heat from the PV to the coolant (A. Powell, personal communication, November 7, 2023). A high surface contact area between the PV and water block is necessary to ensure consistent cooling across the PV to mitigate risks of delamination (Laha et al., 2021). In this paper, an aluminum container spans the rear of a PV, as shown in Figure 1, with tapering towards the water recirculation port(s) to direct coolant in the proper outflow direction. Other materials, including copper and stainless steel, were considered for use in the backplate but were deemed to be too expensive for practical application.

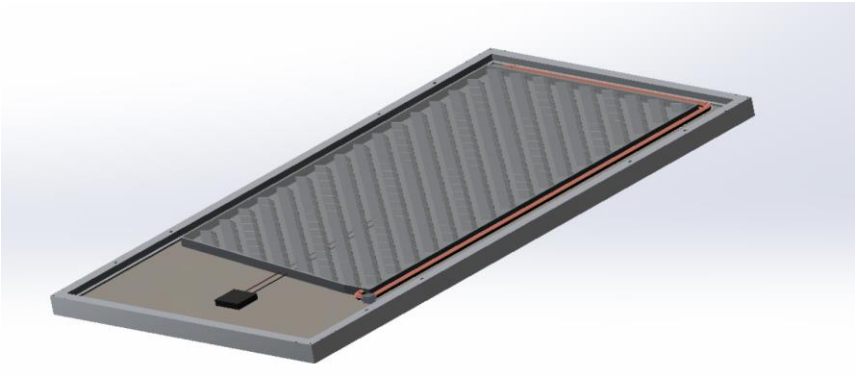

Figure 1. SolidWorks model of aluminum water block on the rear of a PV. The coolant intake can be found at the top left of the model and the outlet at the bottom right. This model is the first iteration used in the *Finite Element Analysis* section.

Water recirculation occurred with the help of a small aquarium pump and flexible vinyl tubing. After flowing through the block, water returns to the top where it flows back through. While the water flows through the aluminum container, it flows around angled aluminum fins, arranged in Figure 2, which aid in the heat distribution into the coolant (Terashima et al., 2023; Zubeer & Ali, 2022). Using angled fins was hypothesized to allow for more effective heat transfer while promoting smooth coolant flow. The top of the block was sealed with another sheet of aluminum.

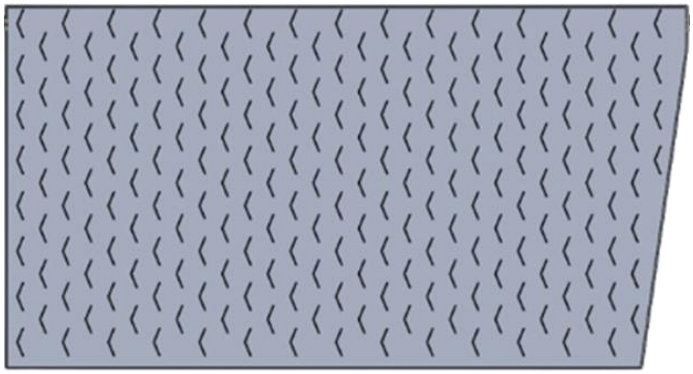

Figure 2. SolidWorks model of aluminum water block with angled fins. This model is the first iteration used in the *Finite Element Analysis* section.

2.3.2 TEG powered water recirculation

Pumps used in water cooling systems can draw somewhere in the range of 12 volts and 3 amps (Chanphavong et al., 2022). Resultantly, using PVs to power their own cooling reduces their net power output. The use of thermoelectric generators is proposed to offset this power draw. Thermoelectric generators, otherwise known as Peltier modules in the Seebeck mode, are devices that convert heat energy into electrical energy (Jaziri et al., 2020). In this model, 10 TEGs were placed on the rear of the panel, above the water block modeled in Figure 1. The power output of these TEGs could then be wired directly to the power input of the recirculation pump so that the TEGs supply or supplement the pump's power draw. Heat sinks were placed on the cold side of the TEGs to help maintain a temperature

contrast between the hot and cold sides of the TEGs. Data from a previous study suggests that TEGs placed on the rear of a panel can produce electricity and reduce panel temperatures (Akal & Türk, 2022). This same logic is applicable to the proposed apparatus and were used to supplement the power for the recirculation pump. As the temperatures of the PV lower, so will the output voltage of the TEG, reducing the speed of the pump. A reduction in pump speed is acceptable because once the panel is cooler, it requires less cooling and lower coolant flow rates.

2.2.3 All in one PV cooling apparatus

The aluminum backplate was fixed to the rear of the panel, assuring full contact with the PV back panel. The recirculation tubing was attached to the water block with custom fittings and to barb fittings present on the pump. The TEGs were fixed to the upper portion of the PV with the help of a silicon thermal glue to aid in the transfer of heat from the PV to the TEGs. The same glue was used to adhere aluminum heat sinks to the cold sides of the TEGs (Alktranee & Péter, 2023). Once put together, the PV-TEG (photovoltaic/thermoelectric generator system) was put into the testing simulator for data collection.

2.4 Finite Element Analysis

To fully understand the interactions between the flowing coolant and the PV, computer-based flow simulations were conducted. SolidWorks Flow Simulation was used to model the fluid dynamics and thermodynamics involved in the cooling block. This software was not used to simulate any interactions within the PV; it takes only an input heat from the aluminum plate (70 Celcius), which is adhered to the rear of the PV and simulates the heat transfer from the plate, through the coolant and to the other side of the water block.

In the final iteration, the coolant (water) enters the PV water block through 5 intake holes positioned at the top and flows through a series of angled aluminum fins until it is directed to 5 lower exit holes placed directly below the intakes (see Figure 3). At the intakes, the water enters at a flow rate comparable to that of a small aquarium pump (240L/min divided amongst the intakes). The bounds of the flow model end at the exit hole. In addition, the mesh size (density of measuring points in the model) was reduced from the maximum with minimal impact on model accuracy to cut down on simulation duration (Laha et al., 2021).

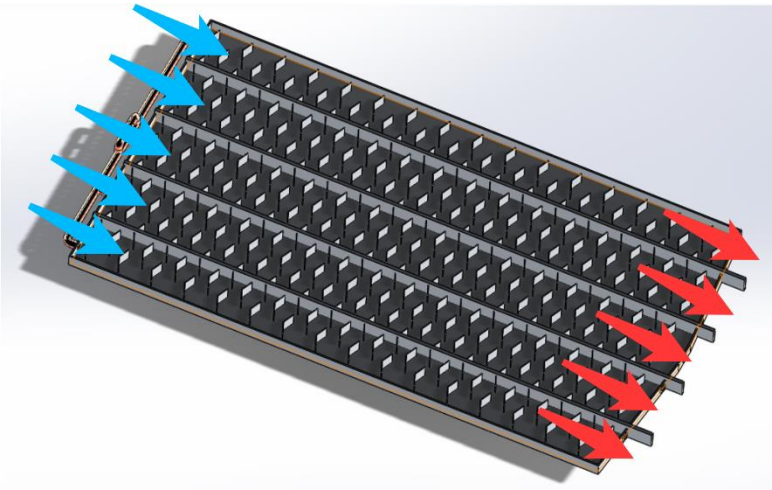

Figure 3. SolidWorks model of aluminum water block on the rear of a PV. Five intakes can be seen at the top of the water block (blue arrows), four dividers can be seen in the block and five outlets can be seen at the bottom of the block (red arrows). This model is the fourth and final iteration used in the *Finite Element Analysis* section.

The results of the model include coolant pressure, water block pressure, coolant temperature, water block wall temperature, water block fin temperature, coolant velocity, and coolant turbulence. These factors were analyzed, and the model adjusted to optimize the heat transfer from the PV

backplate to the coolant. The desired results of the flow simulation include uniform coolant flow and temperature distribution to both remove heat and prevent delamination (Laha et al., 2021).

2.5 Physical Simulation

In order to truly understand the effectiveness of the proposed cooling system, it must be tested in a physical environment. In response to outdoor temperatures well below freezing during the testing period, the sun was simulated indoors with an array of halogen light bulbs. A panel was placed above this array to allow for heat and radiant energy from the bulbs to travel upwards to the PV. A control group used this setup without modification whereas the modified group was fitted with a physical representation of the backplate discussed in *Finite Element Analysis*.

The solar simulator consists of 24, 72W halogen light bulbs wired in parallel at 120V. The array was put in a 6 by 4 light bulb format where every two rows of four light bulbs (8 bulbs, 576W) were wired to 600W dimmer switches to allow for variable light intensity. The dimmer switches were wired in parallel to a power cord which was plugged into a 20A, 120V (2400W) outlet. This design was produced with the help of Shaun Lindgren from Lindgren Electric who advised on safe electricity practices and aided in the overall wiring. In addition to power cables running through the system, ground cables were run through each octagon box (the containers below the bulb mounts) to ground all conductive elements of the system. If any parts of the system become live, a short will trip a circuit breaker and disconnect the electricity. Once operational, a PV was placed above the lights where the radiant energy was converted to electrical energy via the photovoltaic effect. With most of the 1728W of power provided to the bulbs, the rest of it is emitted as radiant energy which travels to the surface of the PV.

This system has been engineered to be both safe and effective. See Figure 4 for a visualization of this model.

Figure 4. The array of 24, 72W halogen light bulbs used to provide radiant energy and heat to the PV.

Once the lighting system was set up, the water block was constructed and fitted to the rear of the panel with one 3W pump sending coolant to the five intakes and collecting it in a container to reuse. The coolant was cooled with freshly collected snow, to simulate a somewhat extreme geothermal cooling system. Above the water block, ten thermoelectric generators were placed and fitted with their own heat sinks (see Figure 5). The panel apparatus was angled parallel to the lights to simulate a zero-degree (perpendicular) angle of incidence. This angle of incidence correlates to the maximum irradiance as is justified by the Cosine Law where E is the incidence energy, E_0 is the perpendicular incidence energy and θ would be the incidence angle (Smith, N. A., 2003).

$$E = E_0 \cos\theta$$

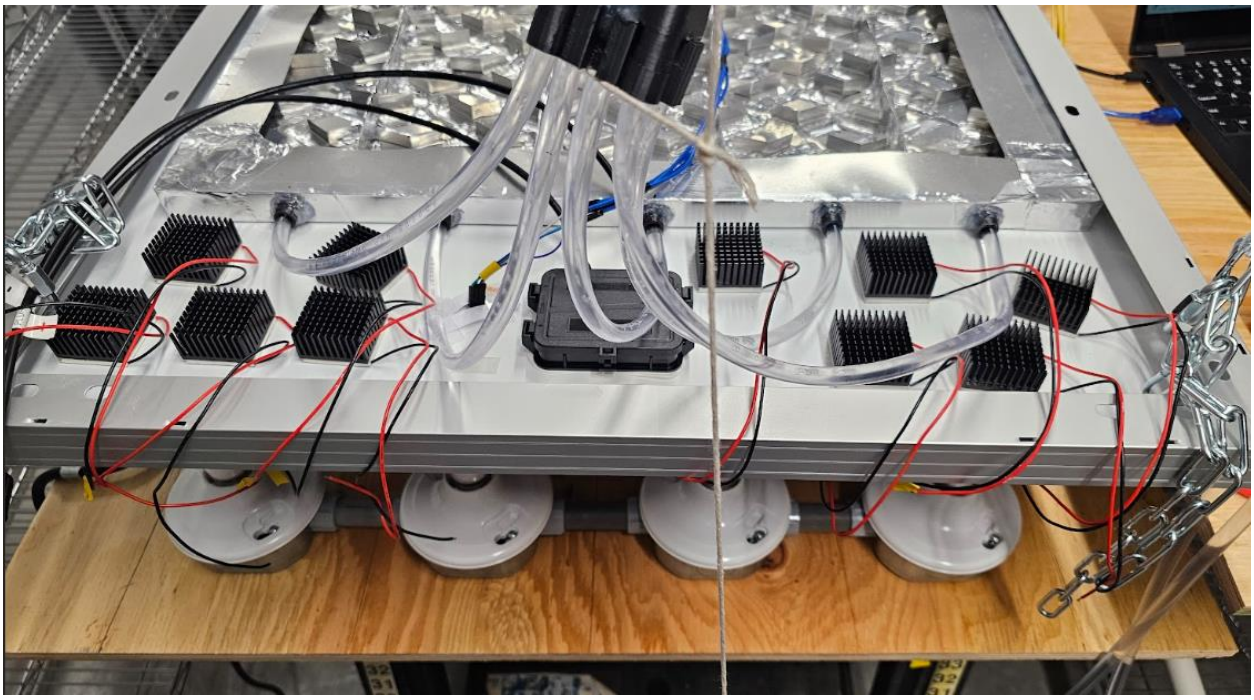

Figure 5. Image of TEGs fitted with heat sinks and water block attached to the rear of the PV.

Once positioned, the Arduino data collection system was set up with 3 temperature probes on the front glass of the PV, and three temperature probes on the rear. Additionally, a light sensor was placed on the surface of the PV to find the lux (lumens per meter) that hit the PV. These sensors collected data every five minutes for the duration of the 120-minute testing period, see figure 6 for a visualization of the Arduino system. Additionally, every five minutes, the power outputs of the PV and thermoelectric generators were measured and the power consumption of the pump logged. The control group experienced all of the same conditions and data collection methods with the exception of thermoelectric and pump data collection as the control model had neither.

Figure 6. (Right) Image of the rear probes on the top of the PV. (Left) Image of probes on the front glass of the PV.

2.6 Statistical Analysis

For verifying improvement in the homogeneity of coolant flow and difference in temperatures in the SolidWorks Flow Simulation and the difference in PV temperatures, f-tests were run. F-tests compare variances and are perfect to verify a reduction in variances in PV temperature and coolant flow. A lower variation signifies an improvement in coolant uniformity. Following physical testing, t-tests were run to check whether the system increased PV output and decreased temperatures by a statistically significant amount. The alpha value used for all significance testing was 0.05.

Section 3: Results

Two separate result categories were considered during the completion of this project. Firstly, finite element modeling on SolidWorks Flow Simulation allowed for the understanding of coolant flow patterns and thermal interactions with the PV. Analyzed data includes coolant temperatures, and

velocity direction and intensity. Then, physical simulation allowed for a real-world test to analyze the system's functionality and impacts on PV power output. Analysis for the real-world simulation considers temperatures at 6 locations, light intensity, the power draw of the recirculation pump, and power outputs of both the PVs and TEGs.

3.1 Finite Element Analysis

SolidWorks Flow Simulation was used to model the fluid dynamics and thermodynamics involved in the cooling block. An equitable distribution of coolant temperatures was desired in these experiments along with consistent velocity patterns to reduce the risk of hotspots and resultantly, delamination of the PV (Laha et al., 2021).

3.1.1 Iteration 1:

The first iteration of the cooling block utilized a design aiming to encourage cross container water flow by placing the intake and outtake on opposing sides. The intake was placed at the top left of the block whereas the outtake was placed at the end of a tapered runoff at the bottom right of the water block. Within the water block were 120-degree, angled aluminum fins, see Figure 7. Lids (imaginary seals) were placed at the intake of and outtake of the water block and using those lids, boundary conditions were established. The upper lid was set to incoming volume at 240L/hour whereas the bottom lid was set to environmental pressure to allow water to leave naturally. Gravity was set to simulate a 45-degree angling of the system, to simulate postponement on a rooftop. Incoming water/coolant was set to 10 degrees Celsius to simulate geothermally cooled coolant. The simulation began with a mesh size of 5, measuring temperature, fluid temperature, solid temperature, fluid turbulence, and fluid velocity.

Figure 7. SolidWorks model of aluminum water block on the rear of a PV. An intake can be found at the top of the PV and an exhaust at the bottom of the PV.

Since the water intake was on the left most side, the highest flow and lowest coolant temperatures were on the left side, see Figure 8. The coolant on the right side was left relatively stagnant and heated up significantly. The coolant temperature had a standard deviation of 5.549 Celsius and the coolant velocity had a standard deviation of 0.0168 m/s, both baselines for the following iterations.

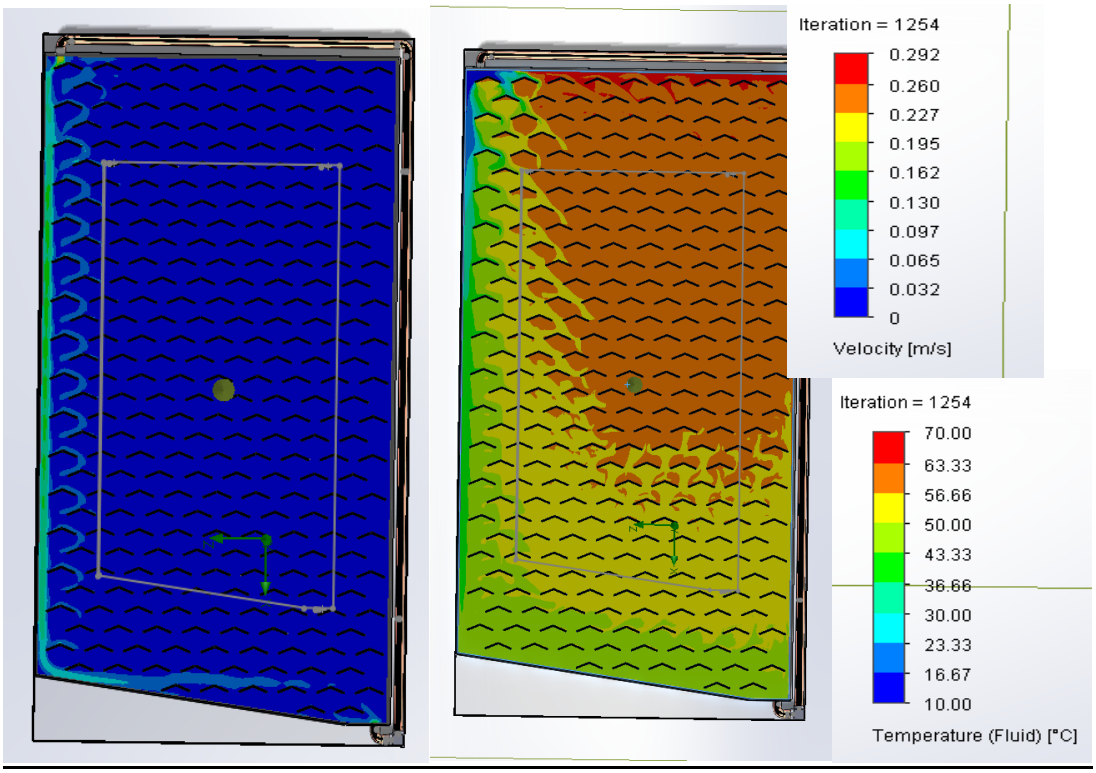

Figure 8. (Left) velocity cut plot where warmer colors represent higher coolant velocities. (Middle) temperature cut plot where warmer colors represent higher coolant temperatures. The figure shows the water block on its side, the simulation orientation can be seen in Figure 8. A key can be found at the right side.

3.1.2 Iteration 2:

The second iteration utilized the same simulation parameters as the first simulation but divided the 240L/hour pump flow rate into five intakes as opposed to one, see Figure 9. The intended result was an equitable distribution of coolant flow, meaning the coolant traveled to all parts of the block and collected heat energy from all parts of the block, relatively uniformly. This would result in relatively uniform coolant temperatures with a slight increase in coolant temperature expected towards the bottom as the coolant increases in temperature during its travel towards the bottom of the water block. The simulation was started at a mesh size of 3, to reduce simulation duration at a minimal expense of model accuracy (Laha et al., 2021).

Figure 9. Model of the aluminum water block on the rear of a PV with five intakes pictured on the top of the model and one exhaust pictured at the bottom of the model. The right side represents the lower half of the PV.

Results suggested an improvement in velocity and temperature distributions with respective standard deviations of 0.0121 m/s and 4.752 Celsius but a new issue arose with the inclusion of 4 additional intakes, over pressurization. Over pressurization occurred as coolant was pumped into the system and was unable to leave, as a result of an inadequate coolant outlet system. Coolant could not flow out of the system fast enough, so it recirculated back to the top of the block. As hot coolant returned to the top of the water block, it created major hotspots. As a result, half of the coolant (the coolant flowing downwards from the intakes) had acceptable flow patterns including acceptable

directions whereas the other half recirculated without leaving the block, creating intense hotspots and undesirable flow directions, see Figure 10.

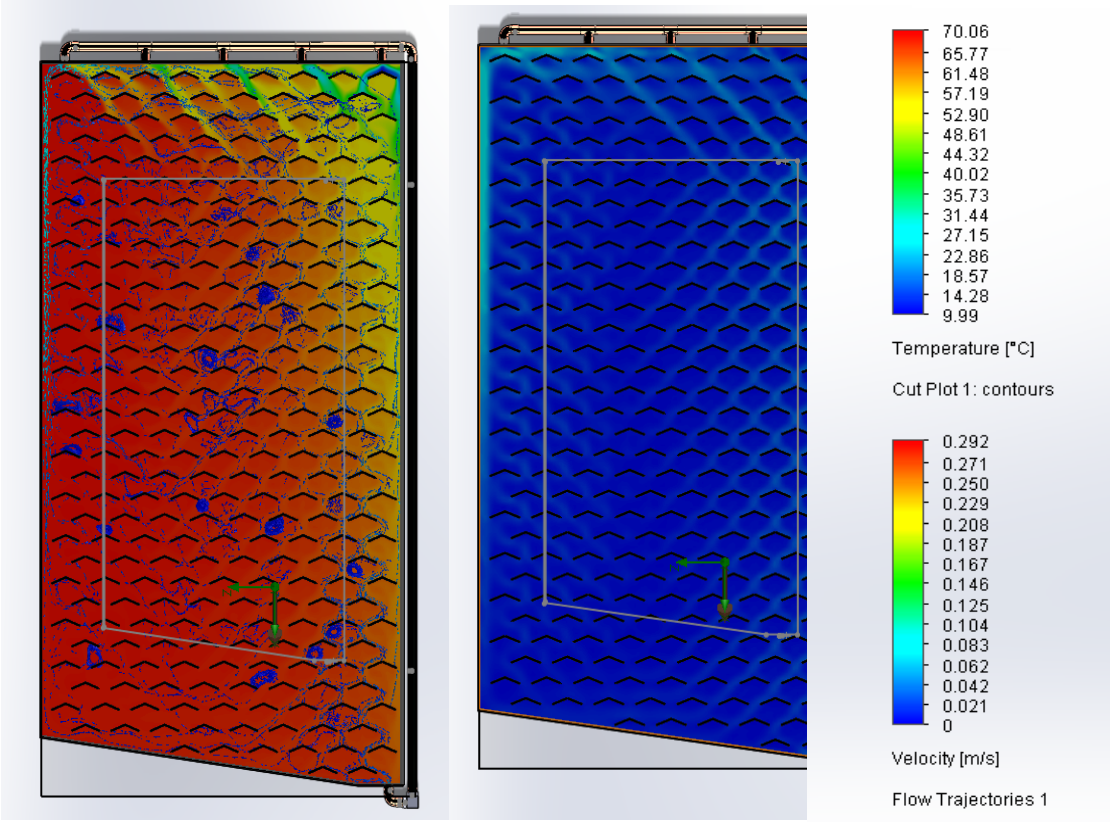

Figure 10. (Left) Cut plot modeling coolant temperature; small arrows can be seen that represent coolant velocity. (Middle) Cut plot modeling coolant velocity. Warmer colors represent higher velocities. Note that the velocities pictured at the left side of the apparatus are traveling upwards, against gravity. A key for both can be found at right.

3.1.3 Iteration 3:

In iteration 3, the outlet's diameter was enlarged to the exact depth of the water block and centralized with tapering directing flow towards the center of the block. An identical simulation was run with these adjustments and results showed little improvement from the prior test. The temperature standard deviation increased to 13.5404 Celsius, whereas the velocity standard deviation decreased

again to 0.0051 m/s. Over pressurization was still prevalent and created a similar effect displayed in the second iteration, leaving a large hotspot consuming the right half of the block, see Figure 11.

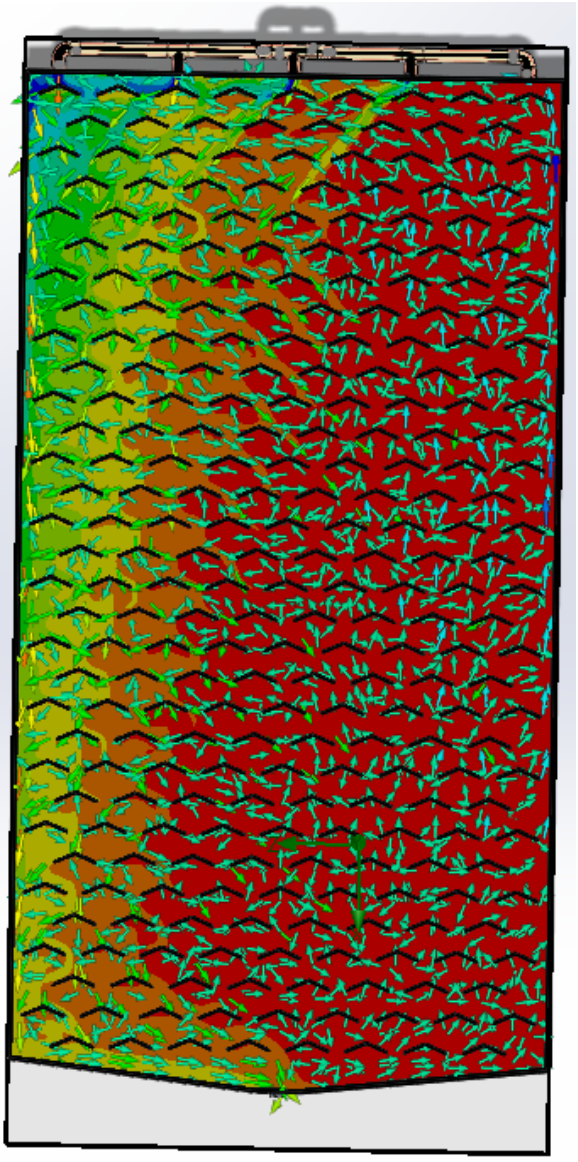

Figure 11. Cut plot modeling coolant velocity and temperature. Arrows represent coolant velocity and background gradients represent coolant temperature. Warmer colors represent higher velocities and temperatures. Note that the velocities pictured at the bottom of the image, the right side of the apparatus are heading upwards, against gravity.

3.1.4 Iteration 4:

In Iteration 4, four lower exhausts were added with four dividers splitting the apparatus into 5 sections, each with one intake and one exhaust, see Figure 12. The intention was for narrower channels to encourage more consistent flow patterns and more exhausts to balance the incoming water flow with output capabilities. An identical simulation was run with these changes made to the apparatus and the mesh size reduced to 2 to both preserve model accuracy but reduce simulation duration. Reduction in simulation duration was key as the addition of more outlets sparked a higher computational demand and increased the testing duration dramatically.

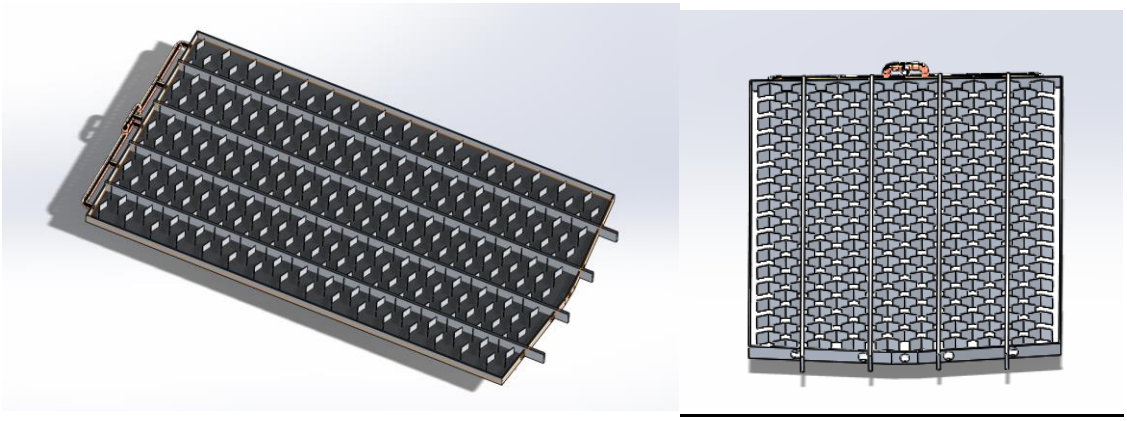

Figure 12. Diagram of apparatus used in Iteration 4. 5 intakes can be seen on the left side of the image on the left, 4 dividers can be seen in the center of both images and five exhausts are located at the right side of the image on the left or the bottom of the image on the right (bottom of apparatus).

The results of this trial satisfied the expectations for this model with highly equalized flow rates and temperatures, see Figure 13. The standard deviations for the temperature and velocity dropped to 2.4667 Celsius and 0.0030 m/s, lower than all previous trials. This iteration was the final iteration and this design was moved forward to physical testing.

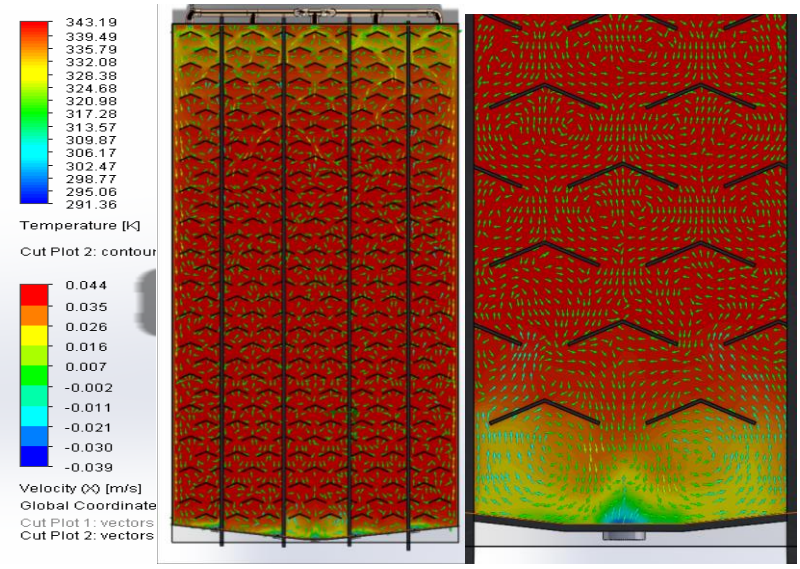

Figure 13. Flow Simulation results where arrows represent coolant velocity and the background gradient represents coolant temperature. The image on the right is a zoomed in version of the bottom portion of the image in the center. A key can be found on the left side.

3.2 Physical Simulation

Physical simulation occurred over the span of 120 minutes and analyzed the temperatures of the PV, power outputs of a control PV and a PV equipped with the water block designed in the fourth and final iteration of the finite element analysis. Each panel was tested independently with average ambient temperatures of 16-18°C for both the control and modified PV and average relative humidities of 42% for both as well. During testing the average power output of the control PV was 46.15W whereas the average power output of the modified PV was 50.85W, see Figure 14. The modified PV showed a 10.18% increase in power output. This signifies an approximate 10.18% increase in efficiency. The 10 TEGs produced a combined average of 0.016W while the pump drew an average of 6W. Thus, the net

draw of the pump-TEG combination was 5.98W and the TEGs were able to subsidize 0.26% of the pump's power draw.

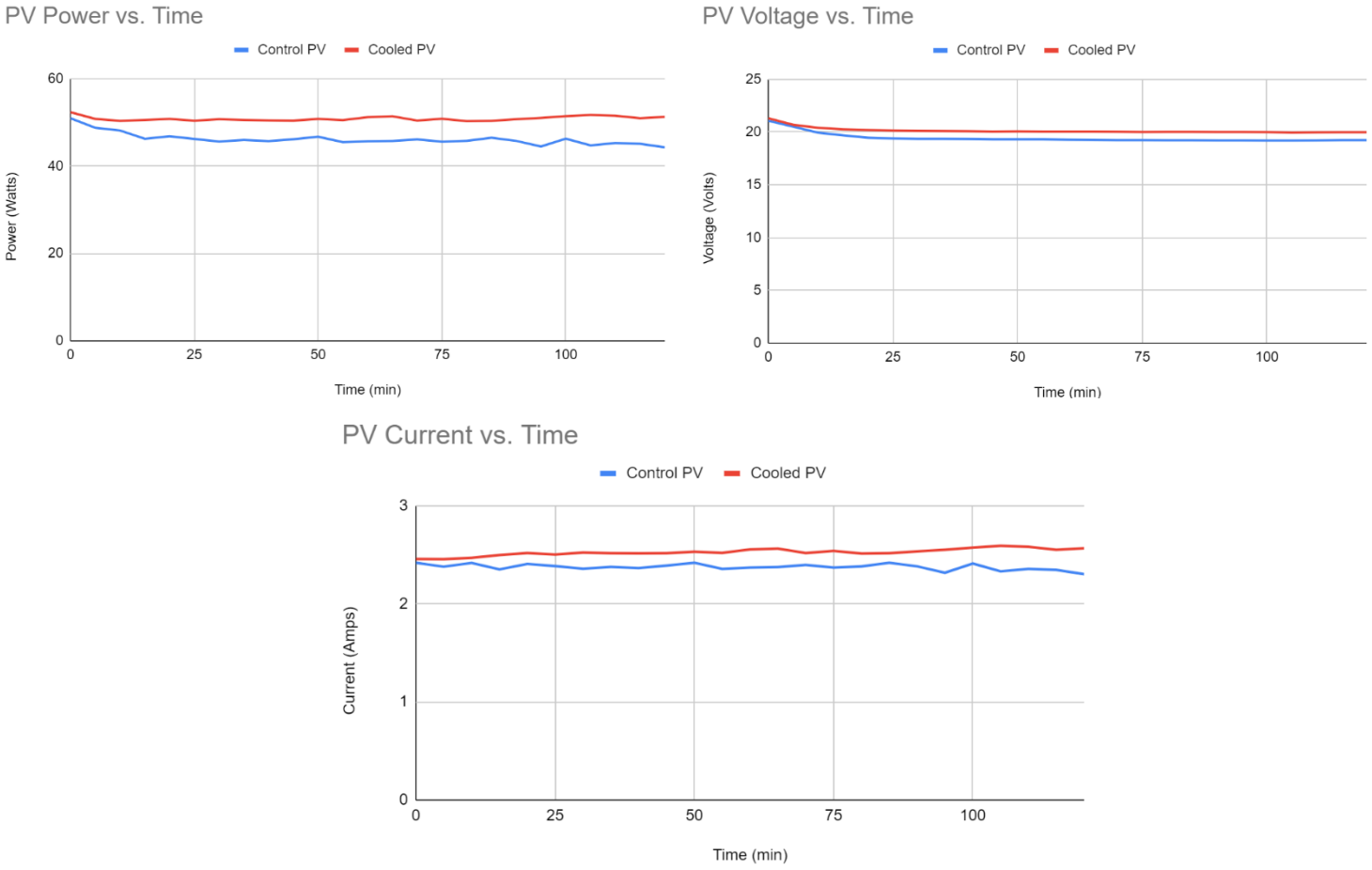

Figure 14. (Top-left) Graph depicting the power output of the control PV and the cooled PV over the course of 120 minutes. (Top-right) Graph depicting the voltage produced by the control PV and the cooled PV over the course of 120 minutes. (Bottom) Graph depicting the current produced by the control PV and the cooled PV over the course of 120 minutes.

The modified PV's glass temperatures measured at an average of 42.49°C whereas the rear of the PV measured at an average of 33.03°C. The control PV had a glass temperature of 52.37°C and a rear

temperature of 39.35°C. The modified PV saw a 18.87% reduction in glass temperature and a 16.07% reduction in rear temperature, see figure 15.

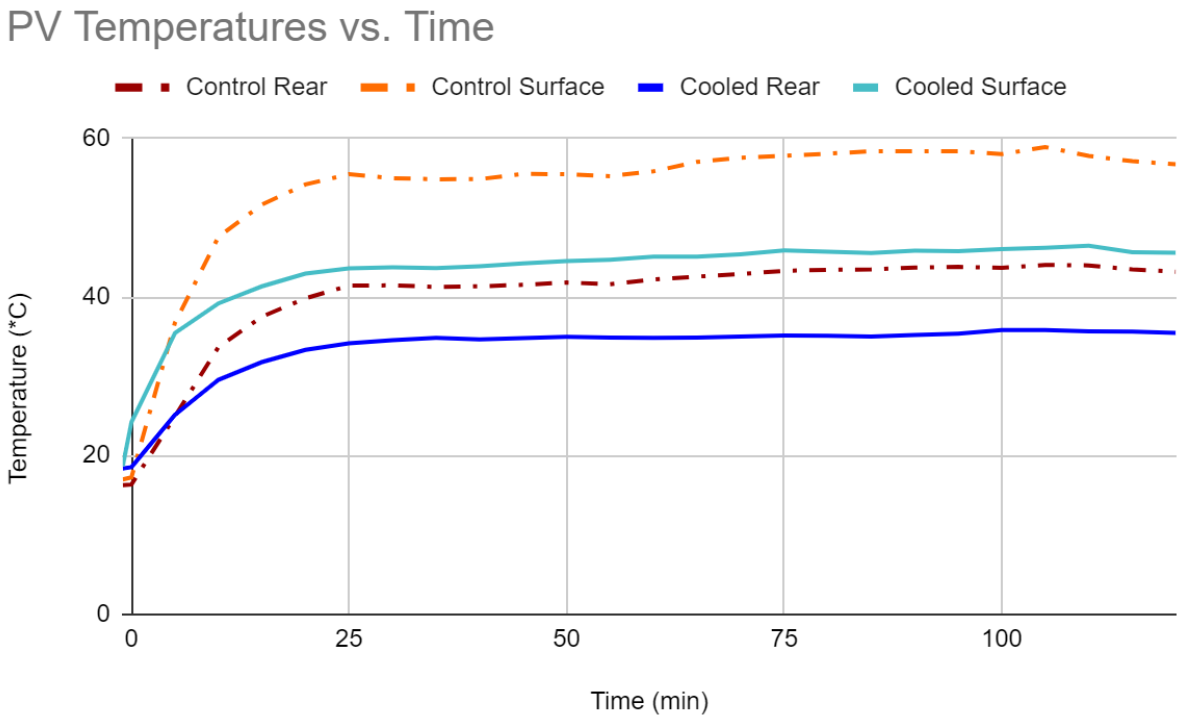

Figure 15. Graph of PV temperatures vs. time where the PV surface is the glass.

Section 4: Discussion

4.1: SolidWorks Flow Simulation

The results of the SolidWorks Flow Simulations signified significant improvement in coolant flow patterns. When compared to the initial iteration, the final iteration showed a 55.55% reduction in coolant temperature standard deviation with an 81.86% reduction in coolant velocity standard deviation. Both were proven significant with all p-values less than 2.35E-76 when data was run with f-tests. F-tests were used as they check for significant differences in variance which is just the square root of standard deviation. This reduction in standard deviations and consequently, variance, signifies

significant improvement in the uniformity of coolant flow and the homogeneity of coolant temperatures. The uniformity of coolant velocity was targeted to prevent dead zones and higher velocity flow areas. With more uniform flow, more coolant leaves at roughly the same rate, preventing portions of the coolant from staying in the water block longer than other portions. Thus, the variance/standard deviation of the coolant temperature reduced. Coolant at a more uniform temperature reinforces uniform panel cooling, reducing temperatures while reducing the risk of delamination. The results of the final design reflect this rationale and provided sufficient evidence to move forward to justify the construction of a physical model.

4.2: Physical Simulation

Over the course of designing and executing the physical simulation, many design challenges were overcome to build the simulator and water block including frequent leaks at fluid flow junctions, the equalization flow distribution and the creation of a lighting array in place of in field testing. Solutions involved creating customized fittings for coolant flow junctions, flow splitters and an array of 24, 72W halogen light bulbs. With each challenge overcome, the design of the system was optimized and improved considerably. Upon the completion of the model, the simulator was run.

Following the end of the trial period, it was observed that the cooled PV showed significant improvements in temperature and power output from the control. With coolant kept at roughly 12-13°C, the cooled PV showed a substantial reduction in both surface and rear temperatures when compared to the control. The resulting increase in power output was 10.18% higher than that of the control, increasing the power output by 4.7W on average, supported with paired t-tests for difference of mean with a p-value of 4.09E-15. The pumps used to circulate fluid in the system drew 6W, resulting in a net decrease in efficiency of 2.8% or 1.28W. In the tested model, the pump was not subsidized by

increased output. With a 10.18% increase in efficiency using the cooling system, a 175W solar panel can easily subsidize the draw of the pump. With the achieved efficiency increase, a control group with an output of 175W normal output, for example, would likely find a net increase of 11.82W or 6.76% when fitted with this cooling system.

The relatively low power output achieved from the 175W PVs in both the control and cooled system comes as the irradiation levels of the Halogen bulbs used in the simulation were not as high as those of the sun in STC, which is roughly 1000W/m^2 (Rahman et al., 2023). Additionally, the power output of a PV depends on the wavelength of light which was not identically simulated by the halogen bulbs, further justifying the relatively low output of both PVs (Ramkiran et al., 2020). Even so, when scaled, the net performance increases found in this study represent a major improvement over the scaled control.

The objectives of this study were almost unanimously achieved. The temperatures of the PV were effectively lowered by an average of 8.1°C or 17.67%, see Figure 15. The reduction in glass temperature was supported with a paired t-test for difference of mean with a p-value of 5.59E-11 and the reduction in the rear temperature was supported with a p-value of 5.62E-11. This reduction in temperature is reasoned as the primary cause of the observed increase in PV power output. Even though the cooled system was unable to produce a net power increase, when scaled it was found that this system could easily achieve a net power increase assuming a similar increase in efficiency.

As far as equitable temperature distributions across the cooled PV, temperature standard deviation was increased by roughly 58.6% or 1.85°C as compared to the control. The temperatures recorded from both the back and front of the control PV had an average standard deviation of 3.16°C whereas the cooled PV temperatures had a standard deviation of approximately 5.01°C. While this increase is a slight drawback of this design, they do not pose a significant threat of delamination (Laha et

al., 2021). These results were supported with f-tests to compare glass and rear temperature variances; the respective p-values were 1.11E-02 and 1.88E-02. The stark difference in p-values between physical testing and SolidWorks Flow Simulations can be explained partially by the sample size used as the FEM significance testing used much larger sample sizes. Without the iterative process taken in the form of finite element analysis, it is likely that the standard deviations of the cooled PV temperatures would have been higher.

The thermoelectric generators failed to fully subsidize the pump power draw and were only able to subsidize approximately 0.26% of the pump power. These findings are in agreement with the findings of Akal & Türk (2022). Overall, the TEGs did not provide significant value to the apparatus and for the most part, only increased the expense of the cooling system.

As for the expense and economics of the system, roughly 50 USD in aluminum were used along with 20 USD in tubing, 40 USD in TEGs and heatsinks, and 15 USD in other extraneous components including adhesives and 3D printed fittings. The estimated materials expense comes out to 125USD with the TEGs included and 85USD without the TEGs/heatsinks. With the TEGs, if central New England was the location of implementation, at an average of 3 hours of direct sunlight (Renogy, 2013), and a 0.274 USD per KWh electricity rate (U.S. Energy Information Administration, 2023b), it would take approximately 38 years to pay off the cooling system with only the aforementioned scaled net increase in power output. Without the TEGs, it would take approximately 24 years to pay off. It is evident that this system is not yet economically viable for an economical implementation at a 175W panel. A higher output PV would pay for this system with net improvements much quicker. This system offers a manufacturable design with a fully recyclable backplate.

4.3: Results in Context

The results observed in this paper are comparable to those achieved by Chanphavong et al. (2022) and Shalaby et al. (2021). This study increased the power output by 10.18%, only 2.5% less than the results observed by Rahman et al. (2023), and only 0.5% less than Salehi et al. (2021). In fact, this study reduced the average temperatures of the PV by approximately 1°C less than the study conducted by Chanphavong et al. (2022), while outperforming the reduction in temperatures observed in the study conducted by Alktranee et al. (2023) by close to 3°C. Overall, while this system may not offer unprecedented increases in power output and reductions in PV temperature, it offers a simple, effective, adaptable solution for cooling PVs while providing a unique method for testing PV output.

4.4: Implications of Research

The results of this study offer a glimpse into the potential for a greener planet. Based on the calculations explained in the introduction, if every PV in the United States was equipped with the proposed cooling system, the U.S. would become 0.6% less dependent on fossil fuels and would burn 6.1 million barrels of petroleum liquids less per year. This value is immense and brings a high level of significance to this system. Furthermore, the majority of this system is recyclable and at the end of its lifespan, will not have as much of an impact on the environment as other plastics-based cooling systems. This system is also scalable and adaptable to any rectangular PV, creating the opportunity for mass implementation once made economical. The proposed water block design is simple, with a low environmental impact, offering scalability to various panel sizes and large improvements to PV efficiency.

4.5: Future Research

Future research building off of the findings of this study should take one or more of the following paths: in-field testing of new iterations, improvement of system economics, reduction in pump power draw, or analysis of larger scale implementation. Field testing of new iterations and the analysis of larger scale implementations have a very similar purpose: testing and verifying the real-world practicality of this system and can aid in further defining areas of improvement for this system. Similarly, improving the economics of this system will aid in increasing this system's ability for real world implementation. One of the largest factors stopping large solar farms from implementing cooling systems is the expense. If the system presented in this paper made sense financially for solar users to implement, the U.S. power grid would see large improvements in its renewability. Lastly, one of the largest resistors to increasing the net PV efficiency with a cooling system is the recirculation pump. Future studies should examine new methods or optimize old methods for coolant circulation. This study is not the end of research in PV water cooling, future studies can work to build upon the findings presented in this paper and work to further optimize PV performance.

Section 5: Conclusion

The primary objective of this study was to increase the net efficiency of a PV using an active, closed loop water cooling system and thermoelectric generators. This study put forth a simple, aluminum water block that when paired with a recirculation system and TEGs, could actively cool a PV and consequently increase its efficiency. To design and analyze the coolant behaviors in this system, SolidWorks Flow Simulations were conducted in combination with an iterative process, identifying and addressing the drawbacks of each iteration, putting forth an improved model each time. To test the

water block, a 1728W array of halogen light bulbs was constructed and a panel placed above to simulate thermal and radiant energy transfer. The results of implementing the water block and TEGs into the physical simulation suggest an approximate 17.67% reduction in PV temperatures and a subsequent 10.18% rise in PV efficiency. When scaled to the full performance of a 175W PV and the pump power draw is accounted for, the system was found to be able to produce a net 11.82W more than a control or 6.76%. The observed improvement in performance, if scaled to large solar arrays and farms, could have massive implications for solar profitability and productivity. These findings are a significant step towards both a more economical, adaptable and effective method for cooling PVs and a greener future for the planet.

Section 6: References

Akal, D., & Türk, S. (2022). Increasing energy and exergy efficiency in photovoltaic panels by reducing the surface temperature with thermoelectric generators. *Energy Sources, Part A: Recovery, Utilization, and Environmental Effects, 44*(2), 4062–4082. https://doi.org/10.1080/15567036.2022.2072980

Alktranee, M., & Péter, B. (2023). Energy and exergy analysis for photovoltaic modules cooled by evaporative cooling techniques. *Energy Reports, 9*, 122–132. https://doi.org/10.1016/j.egyr.2022.11.17

Chanphavong, L., Chanthaboune, V., Phommachanh, S., Vilaida, X., & Bounyanite, P. (2022). Enhancement of performance and exergy analysis of a water-cooling solar photovoltaic panel. *Total Environment Research Themes, 3–4*, 100018. https://doi.org/10.1016/j.totert.2022.100018

Gopinath, M., & Marimuthu, R. (2023). PV-TEG output: Comparison with heat sink and graphite sheet as heat dissipators. *Case Studies in Thermal Engineering, 45*, 102935. https://doi.org/10.1016/j.csite.2023.102935

Jaziri, N., Boughamoura, A., Müller, J., Mezghani, B., Tounsi, F., Ismail, M. (2020). A comprehensive review of thermoelectric generators: technologies and common applications. *Energy Reports, 6*(7 Suppl.), 264-287. https://doi.org/10.1016/j.egyr.2019.12.011

Laha, S. K., Sadhu, P. K., Ganguly, A. & Naskar, A. K. (2021). A comparative study on thermal performance of a 3-D model based solar photovoltaic panel through finite element analysis. *Ain Shams Engineering Journal, 13*(2), 101533. https://doi.org/10.1016/j.asej.2021.06.019

Rahman, N. M. A., Haw, L. C., Kamaluddin, K. A., & Abdullah, M. S. I. (2023). Investigating photovoltaic module performance using aluminium heat sink and forced cold-air circulation method in

tropical climate conditions. *Energy Reports, 9*, 2797–2809. https://doi.org/10.1016/j.egyr.2023.01.130

Ramkiran, B., Sundarabalan, C.K. & Sudhakar, K. (2020). Performance evaluation of solar PV module with filters in an outdoor environment. *Case Studies in Thermal Engineering, 21*, 100700. https://doi.org/10.1016/j.csite.2020.100700

Renogy. (2013). *Average Peak Sun Hours by State.* Retrieved 2024, February 8, from https://www.renogy.com/template/files/Average-Peak-Sun-hours-by-State.pdf

Salehi, R., Jahanbakhshi, A., Reza Golzarian, M., & Khojastehpour, M. (2021). Evaluation of solar panel cooling systems using anodized heat sink equipped with thermoelectric module through the parameters of temperature, power and efficiency. *Energy Conversion and Management: X*, 11, 100102. https://doi.org/10.1016/j.ecmx.2021.100102

Shalaby, S. M., Elfakharany, M. K., Moharram, B.M. & Abosheiasha, H. F. (2021). Experimental study on the performance of PV with water cooling. *Energy Reports, 8*(1 Suppl.), 957-961. https://doi.org/10.1016/j.egyr.2021.11.155

Smith, N.A. (2003). 21 - Lighting. *Electrical Engineer's Reference Book, 16*, 1, 3-31. https://doi.org/10.1016/B978-075064637-6/50021-6

U.S. Energy Information Administration. (2023, October 20). *Frequently asked questions (FAQS)*. Retrieved 2023, October 29, from https://www.eia.gov/tools/faqs/index.php

U.S. Energy Information Administration. (2023, November). *Table 5.6.A. Average Price of Electricity to Ultimate Customers by End-Use Sector.* Retrieved 2024, February 8, from https://www.eia.gov/electricity/monthly/epm_table_grapher.php?t=epmt_5_6_a

Zubeer, S. A., & Ali, O. M. (2022). Experimental and numerical study of low concentration and water-cooling effect on PV module performance. *Case Studies in Thermal Engineering, 34*, 102007. https://doi.org/10.1016/j.csite.2022.102007